Modeling the cardiovascular system using a nonlinear additive autoregressive model with exogenous input

M. Riedl,[1] A. Suhrbier,[2] H. Malberg,[2] T. Penzel,[3] G. Bretthauer,[2] J. Kurths,[4,1] and N. Wessel[1]
[1]*Interdisciplinary Center for Dynamics of Complex Systems, University of Potsdam, Potsdam, Germany*
[2]*Institute for Applied Computer Sciences, Forschungszentrum Karlsruhe GmbH (Karlsruhe Research Center), KIT Karlsruhe Institute of Technology, Karlsruhe, Germany*
[3]*Sleep Center, Charité University Hospital, Berlin, Germany*
[4]*Department of Physics, Humboldt Universität zu Berlin, Berlin, Germany*
(Received 25 January 2008; published 24 July 2008)

The parameters of heart rate variability and blood pressure variability have proved to be useful analytical tools in cardiovascular physics and medicine. Model-based analysis of these variabilities additionally leads to new prognostic information about mechanisms behind regulations in the cardiovascular system. In this paper, we analyze the complex interaction between heart rate, systolic blood pressure, and respiration by nonparametric fitted nonlinear additive autoregressive models with external inputs. Therefore, we consider measurements of healthy persons and patients suffering from obstructive sleep apnea syndrome (OSAS), with and without hypertension. It is shown that the proposed nonlinear models are capable of describing short-term fluctuations in heart rate as well as systolic blood pressure significantly better than similar linear ones, which confirms the assumption of nonlinear controlled heart rate and blood pressure. Furthermore, the comparison of the nonlinear and linear approaches reveals that the heart rate and blood pressure variability in healthy subjects is caused by a higher level of noise as well as nonlinearity than in patients suffering from OSAS. The residue analysis points at a further source of heart rate and blood pressure variability in healthy subjects, in addition to heart rate, systolic blood pressure, and respiration. Comparison of the nonlinear models within and among the different groups of subjects suggests the ability to discriminate the cohorts that could lead to a stratification of hypertension risk in OSAS patients.

DOI: 10.1103/PhysRevE.78.011919 PACS number(s): 87.19.Hh, 02.50.Sk, 05.45.Tp

I. INTRODUCTION

The cardiovascular system often shows complicated temporal, spatial, and spatiotemporal behavior which reflects the complex interactions of many different inherent control loops. Many cardiovascular diseases are characterized by dynamical changes. An early diagnosis of these dynamical diseases often is desirable for successful treatment. Therefore, the adequate quantification of the cardiovascular state and/or regulation is essential. Cardiovascular physics is an interdisciplinary research area which deals with the detailed description and classification of the cardiovascular system [1]. Linear and nonlinear analysis of heart rate variability (HRV) and blood pressure variability (BPV) [2–7] as well as baroreflex sensitivity [8,9] have proved to be highly promising indicators for this topic. With their help, the prediction of preeclampsia (life-threatening blood pressure increase during pregnancy) [10] was improved significantly, for instance. Most of the parameters describe the cardiovascular state where additionally nonlinear parameters of cardiovascular physics lead to a more exact description of the complex HRV and BPV [11–14] than linear ones only. The complexity of the signals arises from many different overlapping control loops in the cardiovascular regulation, for example the baroreflex or the renin-angiotensin-aldosteron system.

Another approach to analyzing this complex system is based on modeling of the complex HRV and BPV. The modeling provides insights into the mechanisms of the cardiovascular regulation and the estimated model parameters can be used to quantify the control. Hence, linear modeling approaches [15–18] already resulted in the successful detection of dysfunctions of cardiovascular regulation; however, various typical nonlinear phenomena, e.g., synchronization or amplitude-frequency coupling in the cardiovascular system, have been observed and therefore must be regarded in the modeling process. Cohen *et al.* [19] proposed a nonlinear transformation of the inputs in order to describe known nonlinear phenomena of heart rate, e.g., saturations and threshold effects or hysteresis. In recent years, nonlinear models [20–27] have proved to be very efficient and necessary to explain HRV and BPV. One of these models is a nonlinear additive autoregressive process with exogenous influence (NAARX) which is characterized by not only linear transformations of the several predictors. In different pilot studies [1,23,28], this model has shown its ability to reproduce the linear and some of the nonlinear properties of the HRV, e.g. cardiorespiratory synchronization. We propose a version of this model where two external sources influence the heart rate and the blood pressure, respectively. We investigate whether this model is suitable to describe the complex dynamics of the heart rate as well as the systolic blood pressure. Finally, we examine if the fitted models allow the detection of pathological changes in cardiovascular regulation. The paper is organized as follows. Section II A contains the data collection and the preprocessing. In Sec. II B, we present the nonlinear model and its nonparametric regression. All statistical tests and analytical tools used are explained in Sec. II C. In Sec. III, the results of the nonparametric regression and the analysis of the model are described. Finally, some conclusions are drawn and remarks made in Sec. IV.

II. METHODS

A. Data

We find a typical example of the dynamical changes of the cardiovascular system in patients suffering from obstructive sleep apnea syndrome (OSAS). OSAS is characterized by repeated full or partial closure of the upper airway for more than 10 s during sleep. This disease is associated with a higher risk for the development of hypertension during sleep and in the daytime [29], or stroke [30]. It is assumed that baroreflex (short-term influence of blood pressure on heart rate) impairment, during the night and furthermore in the daytime, is induced by intermittent hypoxia (decreased oxygen saturation through apneas or hypopneas) and cause developing hypertension [31].

To study the influence of OSAS on cardiovascular regulation, three OSAS patients with and three without hypertension (age 44 ± 6 years) are analyzed. To better assess the applicability of the NAARX model, a group of three healthy persons (age 30 ± 8 years) is also considered. The ages of the healthy group and the groups of OSAS patients are not matched, because our study of OSAS is just beginning, and unfortunately there are no data from available healthy volunteers of comparable age. In this study, we first analyze the cardiovascular variability under standardized conditions in the daytime. Night time sleep stage-dependent analyses are out of the scope of this paper and not considered here. For each subject, an electrocardiogram (sampling rate 1000 Hz), continuous blood pressure (via finger cuff of Portapres device model 2, BMI-TNO, Amsterdam, The Netherlands; sampling rate 200 Hz), and respiration curve (via respiratory effort sensors at the chest; sampling rate 10 Hz) are recorded. The persons were awake with relaxed respiration in the supine position. This study was approved by the local ethics committee and all volunteers and patients gave written informal consent.

From the electrocardiogram, the times of the heart beats are determined using appropriate algorithms [32]. Intervals between successive heart beats ($\{B_i\}$ the beat-to-beat-interval) are calculated. The maximum blood pressure value in each beat-to-beat interval is extracted, which leads to the time series of systolic blood pressure on a beat-to-beat basis ($\{S_i\}$, systolic blood pressure). The values of the respiration signal are determined at the times of the heart beats. Due to the smaller sampling rate of the respiration signal compared to the electrocardiogram, this determination is made by interpolation. The result is a time series of respiratory movement on a beat-to-beat basis ($\{R_i\}$ respiration). Artifacts caused by, e.g., premature beats (beats not initialized by the sinus-atrial node) are removed in $\{B_i\}$ by means of an adaptive filter [3] (see [40]) to prevent such phenomena not originating from the autonomous heart rate regulation from influencing the analysis. Parts of the considered time series are shown in Figs. 1 and 2.

B. Modeling

We are interested in understanding short-time fluctuations of the beat-to-beat intervals and systolic blood pressure. Therefore, these variations are described by a discrete model

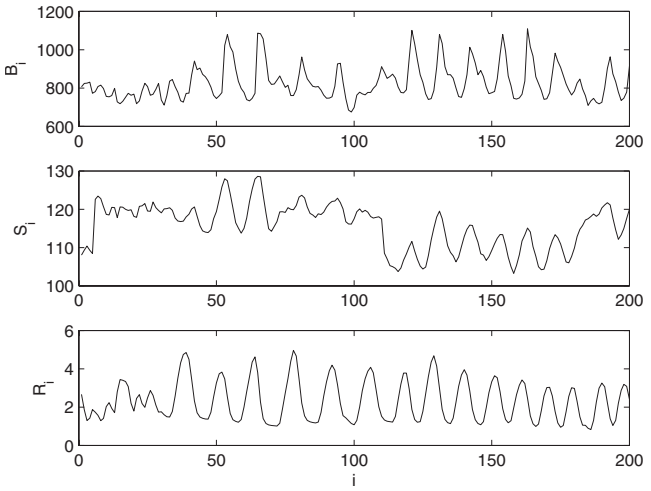

FIG. 1. Extracted time series of the beat-to-beat intervals $\{B_i\}$, the systolic blood pressure on a beat-to-beat basis $\{S_i\}$, and the respiratory movement on a beat-to-beat basis $\{R_i\}$ of the healthy subject H3 in supine position in the daytime.

[15] to take into account the pulsing character of the heart beat and blood pressure on a short time scale. In the cardiovascular system, arterial pressure fluctuations provoke changes in afferent activity of pressure-sensitive receptors, which lead to a change in parasympathetic and sympathetic outflow. This activity of the vegetative nervous system generates changes in beat-to-beat intervals by the cardiac pacemaker. In the model of the heart rate [see Eq. (1)], this so-called baroreflex is modeled by the influence of the previous systolic blood pressure value. Another important source of HRV is respiration, but it is not clear yet whether this cardiorespiratory coordination takes place directly via coupling of the breath control center and the nervous control of the heart rate [33] or indirectly via the baroreflex of respiratory-induced blood pressure variations [15]. Therefore, the model of the heart rate [see Eq. (1)] contains additionally previous

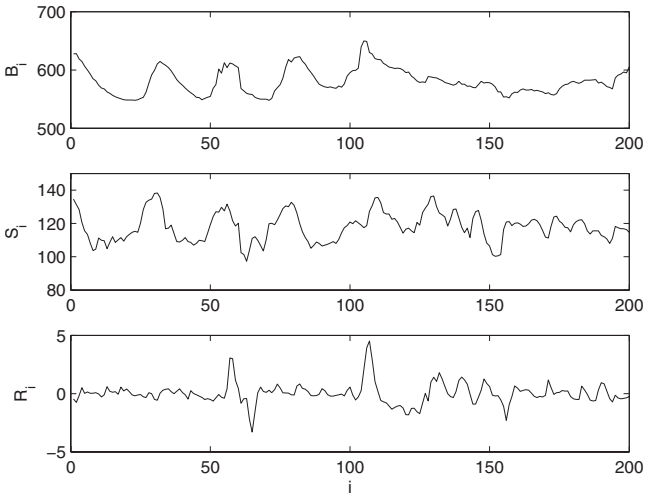

FIG. 2. Extracted time series of the beat-to-beat intervals $\{B_i\}$, the systolic blood pressure on a beat-to-beat basis $\{S_i\}$, and the respiratory movement on a beat-to-beat basis $\{R_i\}$ of the normotensive OSAS patient P1 in supine position in the daytime.

values of the respiration movement, in order to consider both possible cases. Other influences, for instance temperature and the position of the body, are reduced by the standardization of the clinical measurement and/or considered by the autoregressive part of the model and the noise term. On the other hand, the decrease of the heart rate tends to increase the next blood pressure value. This mechanism is assumed to be partly due to the increased filling of the ventricles during a longer beat-to-beat interval which leads to a more forceful contraction of the myocardium (Frank-Starling mechanism). Therefore, the model of systolic blood pressure [see Eq. (2)] contains the previous values of the beat-to-beat interval. The respiratory movement also influences the blood pressure, as aforementioned, and is added to the model Eq. (2). Another influencing source of the BPV is the activity of the vegetative nervous system which controls the peripheral resistance of the vessels. The sympatho-vagal relation is modeled by previous values of the blood pressure and a noise term in the model of BPV [see Eq. (2)]. As the functional relationship of the different cardiovascular values is not clear, we use a nonparametric approach. This will ensure the highest possible flexibility of the model. Other assumptions made in our model are additivity of the influences and the whiteness of the random disturbances. Additivity means that the individual predictors do not interact with each other. Hence, one-dimensional functions can be analyzed instead of multidimensional ones, leading to the following model equations:

$$B_i = \bar{B} + \sum_{j=1}^{p} f_j(B_{i-j}) + g_j(S_{i-j}) + h_j(R_{i-j}) + \epsilon_i, \tag{1}$$

$$S_i = \bar{S} + \sum_{j=1}^{q} k_j(B_{i-j}) + l_j(S_{i-j}) + m_j(R_{i-j}) + \mu_i. \tag{2}$$

$\bar{B}$ and $\bar{S}$ are the mean values of the analyzed time series $\{B_i\}$ and $\{S_i\}$. i ranges from $p+1$ and $q+1$, respectively, to N (length of the time series). p and q denote the orders of the two autoregressive processes. f_j, g_j, h_j, k_j, l_j, and m_j are transformations of the predictors of the models which stand for the weighted portions of the fluctuations in the response variable. $\{\epsilon_i\}$ and $\{\mu_i\}$ are realizations of white noise processes.

This model Eqs. (1) and (2) is fitted nonparametrically using an iterative least-squares algorithm [34], which is called BACKFIT (see Appendix A). A similar procedure, the alternating conditional expectation algorithm, was successfully used for additive nonparametric reconstruction of dynamical systems [35,36]. In contrast to BACKFIT, this algorithm includes a transformation of the response variable. BACKFIT is carried out separately for $\{B_i\}$ and $\{S_i\}$ [see Eqs. (1) and (2)]. Hence, the predictors S_{i-j} and R_{i-j} are external influences in Eq. (1). The same applies to B_{i-j} and R_{i-j} in Eq. (2). BACKFIT uses a nonparametric regression called running line which is a piecewise linear regression. For this kind of smoothing, asymptotic studies yielded an optimum window width of size $N^{4/5}$ [34] which is used in this study as well. Smaller window widths lead to noisy functions which are difficult to explain. On the other hand, for greater window sizes, the bias of the estimated transformation dominates.

The nonlinear models [Eqs. (1) and (2)] are estimated for selected parts of the time series with a length of 200 sample points. This selection reduces trends and excludes nonstationarities in order to guarantee reliable results.

C. Testing

The reliability of the nonlinear shapes of transformations is checked. Therefore, measurements are split into disjoint parts of equal length. If stable cardiovascular regulation is assumed during the measurement, then it is expected that the estimated transformations are quite similar in the different parts. Comparison of the transformations in the different parts will show if the nonlinear shape is reproducible.

The order of the model is determined by a stepwise increase. We study whether the standard deviation of the residue has decreased significantly compared to the previous order. If the standard deviation of the residue is not smaller than 90% of the one in the previous step, then the algorithm is stopped and the order of the previous step is used for modeling.

For comparison, linear autoregressive models with external influences (ARX) are also considered [see Eqs. (3) and (4)]:

$$B_i = \bar{B} + \sum_{j=1}^{p} a_j B_{i-j} + b_j S_{i-j} + c_j R_{i-j} + \epsilon_i', \tag{3}$$

$$S_i = \bar{S} + \sum_{j=1}^{q} r_j B_{i-j} + s_j S_{i-j} + t_j R_{i-j} + \mu_i'. \tag{4}$$

Here a_j, b_j, c_j, r_j, s_j, and t_j are the coefficients of the respective predictors and i ranges from $p+1$ and $q+1$, respectively, to N, where p,q denote the orders of the two autoregressive processes. $\bar{B}$ and $\bar{S}$ are the mean values of the analyzed time series $\{B_i\}$ and $\{S_i\}$. $\{\epsilon_i'\}$ and $\{\mu_i'\}$ denote realizations of white noises. The linear models in Eqs. (3) and (4) are fitted using the MATLAB system identification toolbox [41]. A residual analysis will show whether the NAARX model [Eqs. (1) and (2)] is suited for describing the observed HRV and BPV.

Using the Lagrange multiplier test, it is checked whether additivity of the effects in the model is justified (see Appendix B). This test is performed for both the fitted NAARX [Eqs. (1) and (2)] and ARX models [Eqs. (3) and (4)]. When the test is applied to the ARX model [Eqs. (3) and (4)], the smoothing parameter of the running line in backfitting (see Appendix A) is set to N, the number of random samples, in order to obtain a linear regression over the entire random sample.

Using the Kolmogorov-Smirnov test, it is checked whether the residues are normally distributed with the same mean and variance. Analysis of the autocorrelation function from lag 1 to 10 is supposed to indicate whether the residues may be considered as realizations of independent random variables. Only the first ten lags are studied, as only short-term fluctuations are modeled here. Using an ensemble of 200 simulations of a white noise process, a local confidence

interval of 99% is estimated for the autocorrelation function. For each lag, the upper and lower boundaries of the interval are determined within which 99% of the autocorrelation functions of the ensemble members are ranged. By averaging the upper and lower limits of all ten lags, the confidence limits are obtained. The interval plotted versus the lags represents the confidence band of the autocorrelation function. If the autocorrelation of the individual lags is within this band, the residues may be considered as random. In the case that the autocorrelation of one or several lags is located outside the band, a significant paired dependence of the random variables in $\{\epsilon_i\}$ ($\{\mu_i\}$) [Eqs. (1) and (2)] has to be assumed.

Apart from testing the model assumptions, we check whether the additional expenditure needed for estimating the nonlinear model compared to the linear one is justified. The value of the coefficient of determination Eq. (5) for the NAARX model [Eqs. (1) and (2)] is compared to that for the linear case. The coefficient of determination R^2 is defined as

$$R^2 = \frac{s^2 - s_{\mathrm{res}}^2}{s^2}, \tag{5}$$

where s^2 and s_{res}^2 represent the estimated variance of the modeled variables and the residue. The improvement of the nonlinear approach is also checked by means of an approximated F test (see Appendix A). The null hypothesis of this test is that the fit of the nonlinear model does not represent any significant improvement compared to the linear fit.

For comparison of the linear and nonlinear models, their simulations are also studied. The standard deviation of the random numbers used for this purpose is determined by means of the robust estimator of the mean absolute deviation as follows:

$$s^* = \mathrm{median}(\{|x_i - \hat{x}|\}), \tag{6}$$

where i ranges from 1 to the number of random samples N. $\{|x_i - \hat{x}|\}$ is the set of residues of the regression analyzed. This robust estimator is used, as outliers appear that falsify the estimation of the standard deviation. To ensure the stability of the NAARX model [Eqs. (1) and (2)], the transformations are continued constantly from the boundary points. Newly generated values are transformed by a nearest-neighbor interpolation. As the fits of the NAARX [Eqs. (1) and (2)] and ARX [Eqs. (3) and (4)] models to $\{B_i\}$ and $\{S_i\}$ take place separately, the simulations of these models are also made separately. In the simulations, the original values of the external influences are used. 200 simulations each are generated for the fitted ARX and NAARX models. From these simulations, the confidence bands of the modeled variability are estimated. For each index point, the interval containing 95% of the simulations is searched for. The original time series of the response variable is compared to this confidence band.

III. RESULTS

The fitted NAARX model [Eqs. (1) and (2)] is determined by the estimated transformations of the predictors. A fitted nonlinear model of heart rate fluctuation (see Fig. 1) is shown in Fig. 3. Each curve shows the effect on the beat-to-beat interval of the predictor values. These functions take indeed a nonlinear shape and are distinguishable clearly from a straight line.

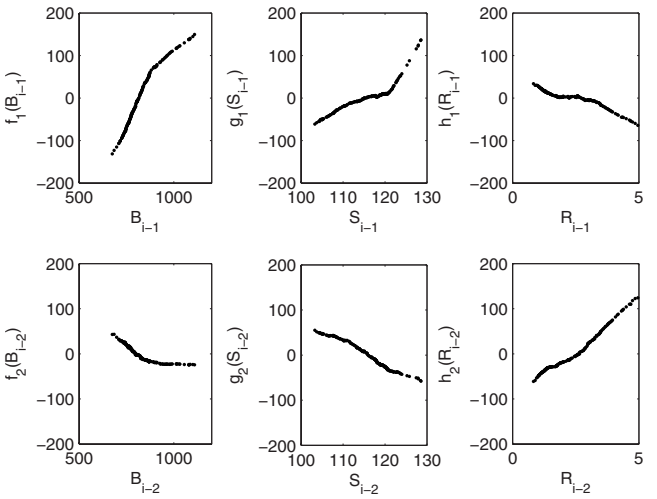

FIG. 3. Estimated transformations of the NAARX model of Eq. (1) to describe the heart rate time series $\{B_i\}$ in Fig. 1.

The number of previous values necessary to describe short-term fluctuations of $\{B_i\}$ and $\{S_i\}$ is determined automatically. It is the order of the model [p,q in Eqs. (1)–(4)], which varies from 1 to 3 (Table I). Only for one case is the value 5, which can be considered as an outlier and results from long-term fluctuations. The comparison of the orders shows the tendency for higher values in the OSAS groups.

We check whether the nonlinear forms of the transformations are reproducible or must be considered as a random effect. Therefore, the measurements are split into disjoint parts of equal length. If it is assumed that the described regulation of the cardiovascular system is stable during the measurement, we expect quite similar curves of the NAARX model [Eqs. (1) and (2)] for the different parts. The resulting curves are shown in Fig. 4 for instance. The horizontal shifts of the functions result from different mean values of the predictor in the different parts; however, the qualitative shape is unchanged. These findings are confirmed for all considered measurements.

TABLE I. Orders determined automatically for the NAARX model of Eqs. (1) and (2) of the time series $\{B_i\}$ and $\{S_i\}$ of the subjects.

Group	Subject	p	q
Healthy subjects	H1	2	2
	H2	2	2
	H3	1	1
Hypertensive OSAS patients	P2	3	3
	P3	2	2
	P6	2	5
Normotensive OSAS patients	P1	3	2
	P4	1	3
	P5	2	1

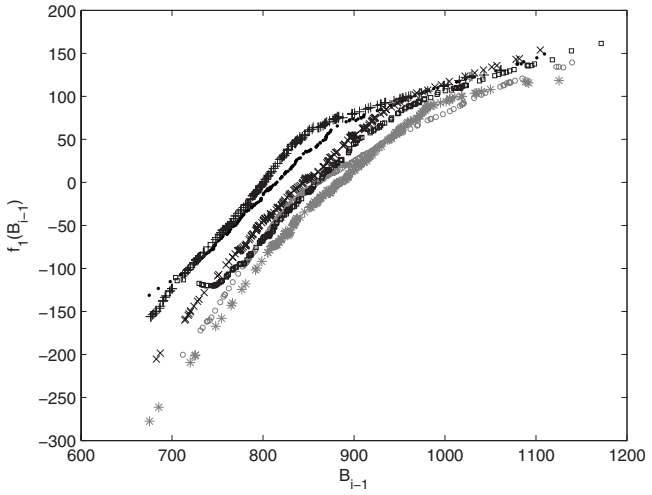

FIG. 4. Estimations of f_1 for successive intervals in time series of healthy person H3. Estimations of intervals with remarkable trends and other nonstationarities are excluded.

The capability of the NAARX model [Eqs. (1) and (2)] to describe HRV and BPV is checked by testing its assumptions. The most important constraint is the additivity of the transformed predictors. It is checked by means of a statistical test (see Appendix B). In only three of 18 cases the additivity must be rejected ($p<0.01$, see Table II). These rejections are not accumulated in any group of the subjects or the models of $\{B_i\}$ and $\{S_i\}$. Therefore, these cases are considered as an effect of multiple testing where the type-1 error of the test leads to false rejections. However, for the linear ARX model [Eqs. (3) and (4)], there are ten rejections of 18 cases, including all cases of the healthy group.

The second assumption of the NAARX model [Eqs. (1) and (2)] is the whiteness of the random terms which we also check. Therefore, the residue must be realizations of identically normal distributed paired independent random variables. The Kolmogorov-Smirnov test is used to verify this condition of normal distributions. By means of this test, we can confirm this condition in all cases.

TABLE II. Decision of the additivity test (see Appendix B) for ARX [Eqs. (3) and (4)] and NAARX [Eqs. (1) and (2)] fits to $\{B_i\}$ and $\{S_i\}$. * labels rejection of assumed additivity. In the cases marked by a dash the hypothesis of additivity can hold. The significance level is 1%.

		ARX		NAARX	
Group	Subject	$\{B_i\}$	$\{S_i\}$	$\{B_i\}$	$\{S_i\}$
Healthy	H1	*	*	—	—
	H2	*	*	*	—
	H3	*	*	—	—
Hypertensive OSAS patients	P2	—	—	—	—
	P3	—	—	—	—
	P6	*	(—[a])	*	(—[a])
Normotensive OSAS patients	P1	—	*	—	—
	P4	—	—	—	—
	P5	*	*	—	*

[a]Linear regression within test was ill conditioned.

TABLE III. Decision obtained by comparing the empirical 99% confidence interval [−0.175,0.175] with the autocorrelation functions of the residues of the ARX [Eqs. (3) and (4)] and NAARX [Eqs. (1) and (2)] fits to $\{B_i\}$ and $\{S_i\}$. If the autocorrelation of one or several lags is located outside the interval, the autocorrelation is considered to be significant (*). Otherwise no significant autocorrelation is labeled by a dash.

		ARX		NAARX	
Group	Subject	$\{B_i\}$	$\{S_i\}$	$\{B_i\}$	$\{S_i\}$
Healthy	H1	*	—	—	—
	H2	*	*	*	*
	H3	*	*	*	*
Hypertensive OSAS patients	P2	—	—	*	—
	P3	—	*	—	—
	P6	*	—	—	—
Normotensive OSAS patients	P1	—	*	*	—
	P4	*	*	—	—
	P5	—	*	—	—

The paired independence of the random variables $\{\epsilon_i\}$ and $\{\mu_i\}$ [Eq. (1) and Eq. (2)] is checked by means of the autocorrelations of the residue (Sec. II B). There are significant autocorrelated residues of the NAARX model [Eqs. (1) and (2)] in six of 18 cases (see Table III). For the linear ARX model [Eqs. (3) and (4)], there are 11 rejections of the paired independence, which are concentrated in the healthy group as well as in the nonlinear model.

The values of R^2, the coefficients of determination [Eq. (5)], of the linear and nonlinear fits are compared in order to determine whether the additional expenditure needed for estimating the nonlinear model is justified (see Table IV). In all cases, R^2 is greater in the NAARX model [Eqs. (1) and (2)] than in the linear one. A Wilcoxon sign test for paired samples confirms a significant increase of the explained variance using the NAARX model ($p<0.01$). The approximated F tests of nonlinearity show that in 16 of 18 cases the nonlinear approach is necessary to describe the short-time fluctuation of heart rate and systolic blood pressure (Table V).

For another way to verify the improvement via the NAARX model [Eqs. (1) and (2)], simulations of the fitted model are studied. An ensemble of 200 realizations is compared to the original time series. Examples of such comparison are presented in Fig. 5. The thin lines mark the upper and lower boundaries of a band that includes 95% of the 200 simulated time series. The original series is drawn by a bold line. In the case of the linear ARX simulations, there are delays of the low-frequency oscillations between simulations and the original series which is illustrated by marked local maxima (vertical lines). These delays occur because the trivial fit, the current value is equal to its predecessor, dominates the linear model. In the case of the fitted nonlinear model [Eqs. (1) and (2)] these delays do not occur. After distinctive disturbances or changing of the dynamic in the time series, simulations of the linear model show transient

TABLE IV. Coefficients of determination R^2 of the NAARX [Eqs. (1) and (2)] and ARX [Eqs. (3) and (4)] models fitted to $\{B_i\}$ and $\{S_i\}$. For paired random samples, the coefficients of determination of both model fits (Wilcoxon sign test) differ significantly: $p<0.01$.

		R^2(NAARX)		R^2(ARX)	
Group	Subject	$\{B_i\}$	$\{S_i\}$	$\{B_i\}$	$\{S_i\}$
Healthy	H1	0.610	0.825	0.402	0.751
	H2	0.641	0.958	0.522	0.927
	H3	0.770	0.958	0.716	0.932
Hypertensive OSAS patients	P2	0.711	0.901	0.643	0.857
	P3	0.947	0.933	0.945	0.921
	P6	0.875	0.930	0.847	0.890
Normotensive OSAS patients	P1	0.944	0.872	0.933	0.832
	P4	0.868	0.844	0.864	0.748
	P5	0.909	0.651	0.890	0.527

behavior (framed in Fig. 5). In the group of healthy people, simulations of the linearly modeled systolic blood pressure diverge (Fig. 5).

IV. SUMMARY AND DISCUSSION

This study shows that the proposed nonlinear model [Eqs. (1) and (2)] is capable of describing short-term fluctuations in heart rate and systolic blood pressure signals significantly better than the linear approximation, which confirms the assumption of nonlinearly controlled heart rate and blood pressure. Additionally, we see a respiratory influence of the heart rate in a direct as well as indirect (via blood pressure fluctuation) fashion (see Fig. 3, right side). Furthermore, the comparison of the nonlinear model [Eqs. (1) and (2)] with the corresponding linear approximation reveals that HRV and BPV in healthy subjects are caused by a higher level of noise as well as nonlinearity than in patients suffering from OSAS. The residue analysis points to a further source of heart rate and blood pressure variability in healthy subjects, in addition to heart rate, systolic blood pressure, and respiration.

The nonparametric fit of the NAARX model [Eqs. (1) and (2)] reveals the nonlinear character of the coupling between the heart rate, systolic blood pressure, and respiratory movement. Obviously the shapes of the functional relations are nonlinear (see Fig. 3). To quantify these forms, a parametrization by means of piecewise linear functions or higher-order polynomials is appropriate. The reliability analysis of the fitted NAARX model [Eqs. (1) and (2)] shows that the non-

TABLE V. Decision of the significance test for nonlinearity[34] for the NAARX fits [Eqs. (1) and (2)]. The asterisk tables significant nonlinear properties.

Group	Subject	B_i NAARX	S_i NAARX
Healthy	H1	*	*
	H2	*	*
	H3	*	*
Hypertensive OSAS subjects	P2	*	*
	P3	—	*
	P6	*	*
Normotensive OSAS patients	P1	*	*
	P4	—	*
	P5	*	*

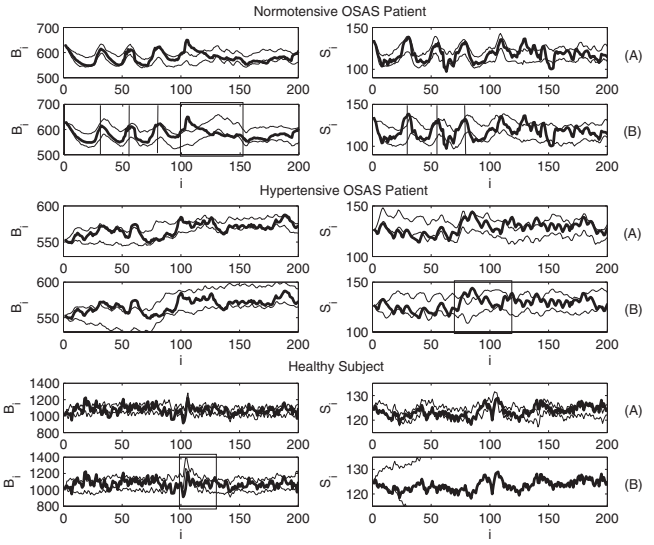

FIG. 5. Comparison of simulations from NAARX [Eqs. (1) and (2)] (a) and ARX [Eqs. (3) and (4)] (b) models for normotensive and hypertensive OSAS patient as well as a healthy subject. Original time series B_i and S_i plotted as bold lines. The thin lines show the local boundaries of the 95% confidence band which is estimated by 200 simulations. Significant delays of the slow oscillation between the original signal and the confidence band of the ARX model are marked by vertical lines located at the local maximum values. The rectangles mark periods of relaxation in the linear simulation. The simulations of S_i in the healthy subject diverge for the linear model (b). [Standard deviation used by simulation is (top) $\sigma_{\mathrm{NAARX}}(B_i)=5.2$, $\sigma_{\mathrm{ARX}}(B_i)=5.6$, $\sigma_{\mathrm{NAARX}}(S_i)=3.1$ and $\sigma_{\mathrm{ARX}}(S_i)=3.5$; (middle) $\sigma_{\mathrm{NAARX}}(B_i)=2.1$, $\sigma_{\mathrm{ARX}}(B_i)=2.2$, $\sigma_{\mathrm{NAARX}}(S_i)=1.6$, and $\sigma_{\mathrm{ARX}}(S_i)=1.7$; (bottom) $\sigma_{\mathrm{NAARX}}(B_i)=32.9$, $\sigma_{\mathrm{ARX}}(B_i)=40.7$, $\sigma_{\mathrm{NAARX}}(S_i)=0.9$, and $\sigma_{\mathrm{ARX}}(S_i)=1.1$].

linear shape of the transformations is reproducible if nonstationarities are excluded from the fit (see Fig. 4). The horizontal shift of the transformations in Fig. 4 results from different mean values of the corresponding predictor; however, the shape is mainly unchanged. These facts indicate that the nonlinear character of the short-term regulation in the cardiovascular system is preserved over a wide range of the mean predictor value. There is a clear direct influence of the respiration on the heart rate (see Fig. 3, right side). An indirect control via blood pressure fluctuations cannot be excluded. We assume that both couplings coexist. The orders p and q tend to higher values in the OSAS groups, which is interpreted as a loss of short-term fluctuations and the increased importance of slower oscillations.

The validity of the NAARX model [Eqs. (1) and (2)] is checked in order to determine whether or not it is suited for describing HRV and BPV. In the case of NAARX modeling, the rejections of additive predictors (asterisks in Table II) are not restricted to a particular group of $\{B_i\}$ and $\{S_i\}$; they may be interpreted as random phenomena caused by multiple testing. Therefore, the most important property is justified in the fitted NAARX model, but fails in many cases of the fitted comparable linear process (see Table II) where the rejections accumulate in the healthy group, because the high level of nonlinear behavior is partly masked as a nonadditive feature. With the proof of additivity a separate analysis of the different couplings between the heart rate, systolic blood pressure, and respiratory movement is possible.

The other assumption of the model, the whiteness of the random term, is satisfied in most of the OSAS patients. Although the normal distribution of the residue is satisfied in all considered cases, there are significant paired autocorrelations of the residues for nearly all healthy persons. Hence, the autocorrelation reflects missing predictors, e.g., the diastolic blood pressure or the oxygen saturation of blood, which must also be considered in the models of heart rate and blood pressure control in healthy subjects. The residue may also be explained by a moving average process. There is no correlation between the predictors and residue; therefore such correction does not lead to a change in the estimated transformations. Thus this modification is not necessary in terms of analysis of interactions between the considered cardiovascular values.

The values of R^2 in Table IV and the simulations show that most of the variance of the original time series can be described by the proposed nonlinear model. The comparison with the corresponding linear model yields a significant improvement of the described variance, which is highest for the healthy person, because the nonlinear deterministic behavior is masked partly as random effects in the linear model. It should be noted that the values of R^2 for OSAS patients are visibly smaller than for the healthy persons, which confirms the experience that the heart rate of healthy subjects is more stochastic than in people suffering from cardiovascular diseases.

The most important limitation of our model is the open loop approach which can lead to cross correlations between the residues of the fits on $\{B_i\}$ and $\{S_i\}$. Another constraint is the necessity for the same order of autoregressive term and the external inputs, where the determination of the order is

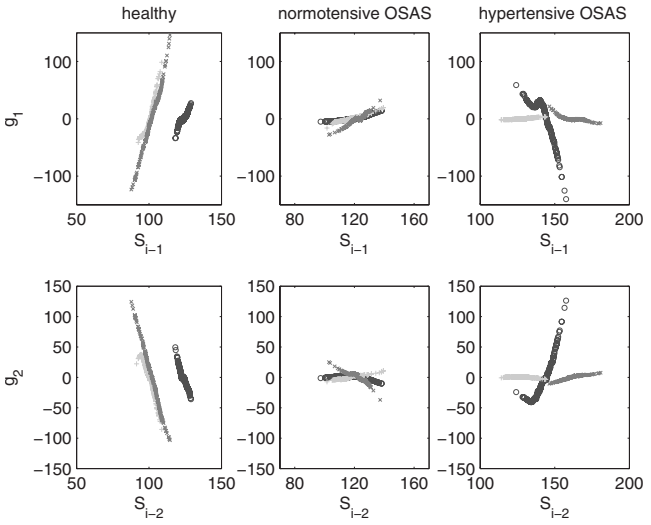

FIG. 6. Transformations of the NAARX model [Eqs. (1) and (2)] of order 2 fitted to the time series $\{B_i\}$. The columns summarize the transformations of the predictors S_{i-1} and S_{i-2} for the subjects of a group. The different persons in the group are given the symbols + (light), ×, and ○ (dark).

sensitive to long-term correlations in the different signals.

In order to show the diagnostic relevance of our approach, the fitted NAARX model [Eqs. (1) and (2)] results are compared inside the different groups of subjects and among them. Therefore, the nonlinear model of order 2 is recalculated for each subject in order to get comparable results. For these fits, g_1 and g_2, the transformations of the first and second predecessor values of blood pressure in Eq. (1), are drawn in Fig. 6. The examples in Fig. 6 reveal that pronounced group-specific properties exist. The slope of the transformation g_1 is remarkably smaller in the normotensive OSAS patients than in the healthy persons, which corresponds to a decreased influence of the systolic blood pressure on the beat-to-beat interval. The changed monotony of this transformation in the group of hypertensive OSAS patients characterizes the pathological regulation of the blood pressure. Therefore, the near-zero slope of g_1 seems to indicate an increased risk for hypertension evoked by the OSAS which demonstrates a possible kind of model-based diagnoses [37]. To validate this guess, more cases must be studied.

The nonlinear shapes of the estimated transformations in the fitted NAARX model (e.g., sharp bends of the transformations) point to different regimes in the cardiovascular regulation. The parametrization of these forms with piecewise linear functions leads to threshold autoregressive models which are able to generate nonlinear phenomena, e.g., amplitude-frequency coupling or synchronization, in combination with external excitation [38]. These phenomena are also found in signals of heart rate and respiratory movement during sleep. Therefore, we hope to describe the complex cardiovascular regulation in sleep, e.g., synchronization between respiration and heart rate or the resetting of the baroreflex, as well.

Finally, the results of the nonlinearity and additivity tests demonstrate the superiority of our nonlinear data-driven

modeling approach over linear ones. Moreover, the fact that we are able to discriminate different patient groups may enable an applicability for clinical OSAS risk stratification.

ACKNOWLEDGMENTS

We acknowledge financial support by the Deutsche Forschungsgemeinschaft Grants No. KU-837/20-2, No. KU-837/23-1, No. BR 1303/8-3, and No. BR 1303/10-1 as well as by the EU Network of Excellence, Grant No. NoE 005137 Biosim and the EU project BRACCIA.

APPENDIX A: FITTING OF ADDITIVE MODELS

The additive model is defined by

$$Y = C + \sum_{j=1}^{p} f_j(X_j) + \epsilon, \tag{A1}$$

where C is a constant value. X_j is the jth predictor, having the effect $f_j(X_j)$ on the influencing variable Y. ϵ is an $N(0,\sigma^2)$ distributed random variable that is stochastically independent of the predictors. If the assumptions for Eq. (A1) are correct, then for any k

$$E\left(Y - \alpha - \sum_{j\neq k}^{p} f_j(X_j)|X_k\right) = f_k(X_k). \tag{A2}$$

By backfitting, the transformations $f_k(X_k)$ are estimated as follows.

(1) Set C to the mean value of Y and choose the starting values of the transformations f_j^0.

(2) For each j, a nonparametric regression of the partial residue is made over the values of the jth predictor [estimation of Eq. (A2)]:

$$\vec{f}_j = S_j\left(\vec{y} - C - \sum_{k\neq j}^{p} \vec{f}_k|\vec{x}_j\right). \tag{A3}$$

Here, S_j is a scatter plot smoother (like a running mean, running line regression, or kernel estimator) for the jth predictor. $(\vec{y},\vec{x}_1,\ldots,\vec{x}_p)$ is a multivariate time series of the random variables $Y,X_1,\ldots,X_p$. $\vec{f}_k$ are the transformed values of the kth predictor.

(3) Continue with step 2 until the estimated transformations no longer change.

For details we refer to p. 82 in Ref. [34].

An approximate F test is used to answer the question whether the estimated transformation is linear or not. Therefore nonparametric fitting is compared to a linear model. The predictors X_j are the same in both cases. s_{lin} and s_{nlin} are the sums of the squared errors of the fitted linear model and the nonparametric regression. Under the zero hypothesis, i.e., estimated transformations of nonparametric regression are linear, the following approximation holds:

$$F = \frac{(s_{\mathrm{lin}} - s_{\mathrm{nlin}})/(\gamma_{\mathrm{nlin}} - \gamma_{\mathrm{lin}})}{s_{\mathrm{nlin}}/(N - \gamma_{\mathrm{nlin}})}. \tag{A4}$$

F is approximately an $F(\gamma_{\mathrm{nlin}}-\gamma_{\mathrm{lin}},N-\gamma_{\mathrm{nlin}})$ distributed random variable. N is the sample number. γ_{lin} and γ_{nlin} are the degrees of freedom of the fitted linear model and nonparametric regression. They can be estimated as follows. When linear smoothers are used, e.g., running line regression, smoothing may be described by a smoothing matrix $\hat{S}$. $\hat{\vec{f}}_y = \hat{S}_x\vec{y}$ holds, where $\vec{y}$ is the sample of the response variable and $\hat{\vec{f}}_y$ the nonparametric regression of Y on X. Based on these matrices, the degrees of freedom of the nonparametric regression can be estimated by

$$\gamma = \sum_j \mathrm{tr}(2\hat{S}_j - \hat{S}_j\hat{S}_j^T) - 1, \tag{A5}$$

where $\mathrm{tr}(X)$ denotes the trace of the matrix X and X^T is the transpose of the matrix. The zero hypothesis must be rejected if the value of F is smaller than the quantile of the distribution $F(\gamma_{\mathrm{nlin}}-\gamma_{\mathrm{lin}},N-\gamma_{\mathrm{nlin}})$ with probability $1-\alpha$ (α is the significance level of the test).

For this test, there is no exact calculation of the distribution of the test statistics. Simulations have shown, however, that it may be used as a rough guideline. For details we refer to p. 65 in Ref. [34].

APPENDIX B: ADDITIVITY TEST

It is assumed that y_i is a realization of a stochastic process, which is stationary and ergodic. According to the zero hypothesis, the time series is based on the nonparametric regression of

$$y_i = \alpha + \sum_{j=1}^{p} [f_j(y_{i-j})] + \sum_{j=1}^{q} [g_j(x_{i-j})] + \epsilon_i. \tag{B1}$$

The alternative is

$$y_i = h(y_{i-1},\ldots,y_{i-p},x_{i-1},\ldots,x_{i-q}) + \epsilon_i. \tag{B2}$$

The test is carried out as follows.

(1) The additive model from the zero hypothesis is fitted to the data by backfitting. The residues $\hat{\epsilon}_i$ of this regression are determined.

(2) Using backfitting, the nonparametric regression of the cross products of second and third order of the predictors is determined over $y_{i-1},\ldots,y_{i-p},x_{i-1},\ldots,x_{i-q}$. The cross products that consist of powers of a predictor only are not considered. For each of the K possible backfittings, the residue e_i is calculated.

(3) The linear regression of $\hat{\epsilon}_i$ over $e_i^1,\ldots,e_i^K$ is determined. The test statistics NR^2 with the sample number N and the coefficient of determination of the regression R^2 [Eq. (5)] are determined.

These test statistics are asymptotically χ^2 distributed with K degrees of freedom. The assumption of additivity must be rejected if the value of the test statistic is smaller than the quantile of the distribution $\chi^2(K)$ with probability $1-\alpha$ (α is the significance level of the test). Details can be found in [39].

[1] N. Wessel, J. Kurths, W. Ditto, and R. Bauernschmitt, Chaos **17**, 015101 (2007).
[2] Task Force of the European Society of Cardiology, the North American Society of Pacing, and Electrophysiology, Circulation **93**, 1043 (1996).
[3] N. Wessel, H. Voss, H. Malberg, C. Ziehmann, H. U. Voss, A. Schirdewan, U. Meyerfeldt, and J. Kurths, Herzschrittmachertherther. Elektrophysiol. **11**, 159 (2000).
[4] K. Kiyono, Z. R. Struzik, N. Aoyagi, F. Togo, and Y. Yamamoto, Phys. Rev. Lett. **95**, 058101 (2005).
[5] N. Wessel, A. Schirdewan, and J. Kurths, Phys. Rev. Lett. **91**, 119801 (2003).
[6] G. McCaffery, T. M. Griffith, K. Naka, M. P. Frennaux, and C. C. Matthai, Phys. Rev. E **65**, 022901 (2002).
[7] N. Wessel, C. Ziehmann, J. Kurths, U. Meyerfeldt, A. Schirdewan, and A. Voss, Phys. Rev. E **61**, 733 (2000).
[8] M. D. Thames, T. Kinugawa, M. L. Smith, and M. E. Dibner-Dunlap, J. Am. Coll. Cardiol. **22**, 56 (1993).
[9] H. Malberg, N. Wessel, A. Hasart, K. J. Osterziel, and A. Voss, Clin. Sci. **102**, 465 (2002).
[10] H. Malberg, R. Bauernschmitt, A. Voss, T. Walther, R. Faber, H. Stepan, and N. Wessel, Chaos **17**, 015113 (2007).
[11] K. Kiyono, Z. R. Struzik, N. Aoyagi, S. Sakata, J. Hayano, and Y. Yamamoto, Phys. Rev. Lett. **93**, 178103 (2004).
[12] N. Marwan, N. Wessel, U. Meyerfeldt, A. Schirdewan, and J. Kurths, Phys. Rev. E **66**, 026702 (2002).
[13] C. Schäfer, M. G. Rosenblum, H. H. Abel, and J. Kurths, Phys. Rev. E **60**, 857 (1999).
[14] A. Porta *et al.*, Chaos **17**, 015117 (2007).
[15] R. W. deBoer, J. M. Karemaker, and J. Strackee, Am. J. Physiol. Heart Circ. Physiol. **253**, 680 (1987).
[16] G. Baselli, S. Cerutti, F. Badilini, L. Biancardi, A. Porta, M. Pagani, F. Lombardi, O. Rimoldi, R. Furlan, and A. Malliani, Med. Biol. Eng. Comput. **32**, 143 (1994).
[17] S. Matsukawa and T. Wáda, Am. J. Physiol. Heart Circ. Physiol. **273**, 478 (1997).
[18] A. Porta, G. Baselli, O. Rimoldi, A. Malliani, and M. Pagani, Am. J. Physiol. Heart Circ. Physiol. **279**, 2558 (2000).
[19] M. A. Cohen and J. A. Taylor, J. Physiol. (London) **542**, 669 (2002).
[20] A. A. Armoundas, K. Ju, N. Iyengar, J. K. Kanters, P. J. Saul, R. J. Cohen, and K. H. Chon, Ann. Biomed. Eng. **30**, 192 (2002).
[21] V. Belozeroff, R. B. Beny, C. S. H. Sassoon, and M. C. K. Khoo, Am. J. Physiol. Heart Circ. Physiol. **282**, 110 (2002).
[22] J. W. Kantelhardt, S. Havlin, and P. C. Ivanov, Europhys. Lett. **62**, 147 (2003).
[23] N. Wessel, H. Malberg, R. Bauernschmitt, A. Schirdewan, and J. Kurths, Med. Biol. Eng. Comput. **44**, 321 (2006).
[24] K. Kotani, Z. R. Struzik, K. Takamasu, H. E. Stanley, and Y. Yamamoto, Phys. Rev. E **72**, 041904 (2005).
[25] S. Bauer, G. Röder, and M. Bär, Chaos **17**, 015104 (2007).
[26] T. Kuusela, Phys. Rev. E **69**, 031916 (2004).
[27] J. J. Zebrowski, K. Grudzinski, T. Buchner, P. Kuklik, J. Gac, G. Gielerak, P. Sanders, and R. Baranowski, Chaos **17**, 015121 (2007).
[28] T. Penzel, N. Wessel, M. Riedl, J. Kantelhardt, S. Rostig, M. Glos, A. Suhrbier, H. Malberg, and I. Fietze, Chaos **17**, 015116 (2007).
[29] P. E. Peppard, T. Young, M. Palta, and J. Skatrud, N. Engl. J. Med. **342**, 1378 (2000).
[30] H. K. Yaggi, J. Concato, W. N. Kernan, J. H. Lichtman, L. M. Brass, and V. Mohsenin, N. Engl. J. Med. **353**, 2034 (2005).
[31] C. J. Lai, C. C. Yang, Y. Y. Hsu, Y. N. Lin, and T. B. Kuo, J. Appl. Physiol. **100**, 1974 (2006).
[32] A. Suhrbier, R. Heringer, T. Walther, H. Malberg, and N. Wessel, Biomed. Tech. **51**, 70 (2006).
[33] P. D. Larsen, E. L. Trent, and D. C. Galletly, Br. J. Anaesth. **82**, 546 (1999).
[34] T. J. Hastie and R. J. Tibshirani, *Generalized Additive Models* (Chapman & Hall, London, 1990).
[35] H. Voss and J. Kurths, Phys. Lett. A **234**, 336 (1997).
[36] M. Abel, K. Ahnert, J. Kurths, and S. Mandelj, Phys. Rev. E **71**, 015203(R) (2005).
[37] J. Prusseit and K. Lehnertz, Phys. Rev. Lett. **98**, 138103 (2007).
[38] H. Tong, *Non-linear Time Series: A Dynamical System Approach* (Oxford Science Publications, Oxford, 1990).
[39] R. Chen, J. S. Liu, and R. S. Tsay, Biometrika **82**, 369 (1996).
[40] http://tocsy.agnld.uni-potsdam.de
[41] Computer code MATLAB (The Math Works, Inc., Natick, ME, USA).